Acta Cryst. (1994). A**50**, 330–337

A Direct Investigation of Thermal Vibrations of Beryllium in Real Space through the Maximum-Entropy Method Applied to Single-Crystal Neutron Diffraction Data

BY M. TAKATA AND M. SAKATA

Department of Applied Physics, Nagoya University, Nagoya 464-01, *Japan*

S. KUMAZAWA

Department of Physics, Science University of Tokyo, Noda, Chiba 278, *Japan*

AND F. K. LARSEN AND B. B. IVERSEN

Department of Chemistry, Aarhus University, DK-8000, *Aarhus C, Denmark*

(*Received* 21 *June* 1993; *accepted* 19 *October* 1993)

Abstract

The thermal vibrations of beryllium metal were determined directly from the nuclear densities obtained by the maximum-entropy method (MEM) using neutron single-crystal data. A high-resolution nuclear density distribution of beryllium was obtained by applying the MEM to the 48 structure factors with $\sin\theta/\lambda < 1.41$ Å^{-1} from a previous study [Larsen, Lehmann & Merisalo (1980). *Acta Cryst.* A**36**, 159–163], which showed small but significant cubic anharmonicity in beryllium by least-squares refinement of the structure factors. In the present study, quartic as well as cubic anharmonicities are clearly visible in the MEM nuclear density. In order to determine anharmonic thermal-vibration parameters, a three-dimensional function was fitted to the MEM nuclear density around the atom site. The one-particle potential was used to model the thermal vibrations up to quartic terms. The least-squares-fit values were $\gamma = -0.306$ eV Å^{-3} for the third- and $\alpha_{40} = -1.02$, $\beta_{20} = 2.95$ and $\gamma_{00} = -3.28$ eV Å^{-4} for the fourth-order anharmonic parameters. Thus, the atomic potential in the basal plane is hardened against the bipyramidal space around the tetrahedral holes of the hexagonal-close-packed structure. It is softened towards the center of the octahedral voids. Least-squares refinement of the MEM nuclear density gives a standard deviation of about 5 for the last digit of the anharmonic parameters. However, there is added uncertainty in the parameters because of the relationship of the reliability of the MEM density distribution to the standard deviations of the measured intensities. Judging from previous studies of the thermal parameters for beryllium based on least-squares refinement of observed structure factors, it is estimated that values determined here for the anharmonic parameters are reliable to the first digit after the decimal point.

1. Introduction

The maximum-entropy method (MEM) yields a high-resolution density distribution from even a limited number of diffraction data, without the use of a structural model (Sakata & Sato, 1990). Since X-rays are diffracted by electrons, MEM analysis of X-ray data can provide the electron-density distribution. Different aspects of the bonding nature in the crystalline state have been displayed in such MEM investigations of the real-space electronic structure for several substances, such as silicon (Sakata & Sato, 1990), CeO_2 (Sakata, Mori, Kumazawa, Takata & Toraya, 1990), TiO_2 (Sakata, Uno, Takata & Mori, 1992), ice (I_h) (Sakata, Takata, Oshizumi, Goto & Hondoh, 1992), CaF_2 and TiO_2 (Sakata, Takata, Kubota, Uno, Kumazawa & Howard, 1992), LiF (Takata, Yamada, Kubota & Sakata, 1992) and beryllium (Takata, Kubota & Sakata, 1993).

For non-magnetic materials, neutrons are predominantly diffracted by the atomic nuclei. MEM analysis of neutron diffraction data therefore yields the nuclear-density distribution, which is equivalent to the point-nuclei distribution smeared by the atomic thermal motions, that is, the thermal smearing function. It is now possible to determine the thermal smearing function even in cases of negative scattering length (Sakata, Uno, Takata & Howard, 1993). Thus, MEM analysis of neutron diffraction data should enable us to investigate thermal vibrational features directly in real space for any crystalline material without using a structural model. The present study examines the capability of direct investigation of atomic thermal vibrations *via* the MEM nuclear-density distribution.

A conventional approach to describing atomic thermal motion is to assume that the vibrations are determined by an effective one-particle potential (OPP), which is expanded according to the atomic

ISSN 0108-7673 ©1994

site symmetry. The corresponding atomic thermal smearing function of real space and the Debye–Waller factor of reciprocal space can be parametrized in terms of the OPP model. Conventionally, the parameters of the OPP model are determined by least-squares fitting of the Debye–Waller factor to X-ray or neutron structure-factor data in reciprocal space. In the present study, the parameters are determined by least-squares fitting of the thermal smearing function to the MEM nuclear-density distribution in real space.

Beryllium is used as a test case. Beryllium metal is very hard and brittle, with a Debye temperature of 1150 K and small thermal vibrations. The mean-square atomic displacement and antisymmetric atomic vibrations in it at room temperature were determined from good single-crystal short-wavelength neutron data of modest extinction by a conventional analysis (Larsen, Lehmann & Merisalo, 1980). It was found to have a small but significant cubic anharmonic thermal-motion component even at room temperature. The main interest of the present study is to understand how far MEM analysis can reveal the existence of anharmonic motion using the same neutron structure-factor data.

2. The MEM analysis

In the previous study (Larsen, Lehmann & Merisalo, 1980), two sets of neutron diffraction data for beryllium were collected at 295 K from two single crystals of volumes 8 and 27 mm^3 with wavelengths of 0.525 and 0.425 Å, respectively. Although the degree of extinction was quite different for the two crystals, the mean-square displacements determined from the two sets of data using full-matrix least-squares refinement of structure factors were almost identical. The smallest values of inverse extinction-correction factors were 0.94 and 0.49 for the crystals of volumes 8 and 27 mm^3, respectively. Ideally extinction-free data is suitable for MEM analysis (Sakato & Sato, 1990). Hence, the former set of data was used for the present MEM analysis. Only the 48 lower-angle reflections up to $\sin\theta/\lambda < 1.41$ $Å^{-1}$ are used in the MEM analysis to avoid most of the added uncertainty coming from the correction for thermal diffuse scattering in the high-order reflections.

Details of the procedure used to obtain the MEM density distributions are given by Sakato & Sato (1990). Their MEM algorithm is based on the formalism of Collins (1982). The MEM analysis was carried out with the computer program *MEED* (Kumazawa, Kubota, Takata, Sakata & Ishibashi, 1993). In the present analysis, the unit cell was divided into $120 \times 120 \times 120$ pixels to ensure good spatial resolution. The unit pixel size becomes $0.019 \times 0.019 \times 0.030$ Å. The total computing time was 727 s for 10 892 iterations with a FACOM VP2600 vector computer. The observed structure factors with their standard deviations and the derived structure factors obtained through the MEM procedure, F_{MEM}, are listed in Table 1.

Table 1. *The list of F_{obs} from a neutron single-crystal diffraction experiment on beryllium (Larsen, Lehmann & Merisalo, 1980) and the corresponding structure factors, F_{MEM}, calculated from the MEM nuclear-density distribution shown in Fig. 1*

H	K	L	F_{obs}	F_{MEM}
0	0	2	−1.51 (3)	−1.46
1	0	1	−1.30 (2)	−1.25
1	0	2	0.738 (9)	0.713
1	0	3	1.22 (2)	1.18
1	1	2	−1.37 (2)	−1.34
2	0	1	1.16 (2)	1.15
0	0	4	1.35 (2)	1.34
2	0	2	0.676 (9)	0.657
1	0	4	−0.653 (9)	−0.649
2	0	3	−1.11 (2)	−1.09
2	1	1	−1.07 (1)	−1.06
1	1	4	1.24 (2)	1.23
2	1	2	0.612 (7)	0.602
1	0	5	−1.05 (1)	−1.05
2	0	4	−0.605(7)	−0.600
2	1	3	1.01 (1)	1.00
3	0	2	−1.15 (1)	−1.14
0	0	6	−1.15 (2)	−1.15
2	0	5	0.97 (1)	0.97
2	1	4	−0.556 (8)	−0.550
1	0	6	0.560 (8)	0.559
2	2	2	−1.04 (2)	−1.05
3	1	1	0.88 (2)	0.90
3	0	4	1.04 (2)	1.04
1	1	6	−1.05 (2)	−1.06
3	1	2	0.52 (1)	0.51
2	1	5	−0.89 (2)	−0.89
2	0	6	0.51 (1)	0.52
3	1	3	−0.85 (2)	−0.86
1	0	7	0.87 (2)	0.88
4	0	1	−0.82 (2)	−0.84
2	2	4	0.94 (2)	0.96
4	0	2	0.46 (1)	0.47
3	1	4	−0.47 (1)	−0.47
2	1	6	0.48 (1)	0.48
4	0	3	0.78 (2)	0.79
2	0	7	−0.80 (2)	−0.81
3	2	1	−0.75 (2)	−0.77
0	0	8	0.92 (3)	0.93
3	0	6	−0.89 (3)	−0.90
3	2	2	0.42 (1)	0.43
1	0	8	−0.44 (1)	−0.45
3	1	5	0.74 (2)	0.76
4	0	4	−0.42 (1)	−0.43
3	2	3	0.71 (2)	0.73
2	1	7	0.73 (2)	0.75
4	1	2	−0.80 (3)	−0.83
1	1	8	0.83 (3)	0.86

3. The MEM nuclear density and the anharmonicities of beryllium

Beryllium metal has a hexagonal-close-packed (h.c.p.) structure. The MEM nuclear-density distributions in the (110) and basal planes are shown in Figs. 1(*a*) and (*b*), respectively. The contours are on a

logarithmic scale. The nuclear density is concentrated in a small region around the presumed atomic sites, with peak maxima of 144.772×10^{-14} m Å^{-3} (187.044 neutrons Å^{-3}). In the interatomic region, the nuclear density is very close to zero (0.034 neutrons Å^{-3}). These very reasonable features for a nuclear-density distribution contrast with the electron-density distribution, as shown in § 7.

The ratio $c/a = 1.568$ for beryllium metal is smaller than the expected value of $c/a = 1.633$ for the h.c.p. hard-sphere model. Concordantly, previous studies (Larsen, Lehmann & Merisalo, 1980; Larsen, Brown, Lehmann, & Merisalo, 1982) found mean-square amplitudes $\langle u_c^2 \rangle < \langle u_a^2 \rangle = \langle u_b^2 \rangle$. In the harmonic approximation, this corresponds to oblate thermal ellipsoids, which give elliptical circular shapes for the thermal smearing function. Obviously, the MEM nuclear densities shown in Fig. 1 are not simple elliptical shapes, indicating the existence of anharmonic vibrations.

In the Fig. 1(*b*) basal plane, a triangular feature is clearly visible. For the harmonic model, nuclear-density contours should be circular in this plane. According to the OPP model, a third-order anharmonic term will distort the effective potential antisymmetrically in the basal plane of the h.c.p. lattice, deforming the equipotential contours into a triangular shape. It is therefore reasonable to interpret the characteristic triangular feature of the MEM nuclear density in the h.c.p. basal plane shown in Fig. 1(*b*) as being caused by third-order anharmonic vibrations. Indeed, third-order anharmonicity for beryllium was observed in previous studies (Merisalo, Järvinen & Kurittu, 1978; Larsen, Lehmann & Merisalo, 1980; Larsen, Brown, Lehmann & Merisalo, 1982).

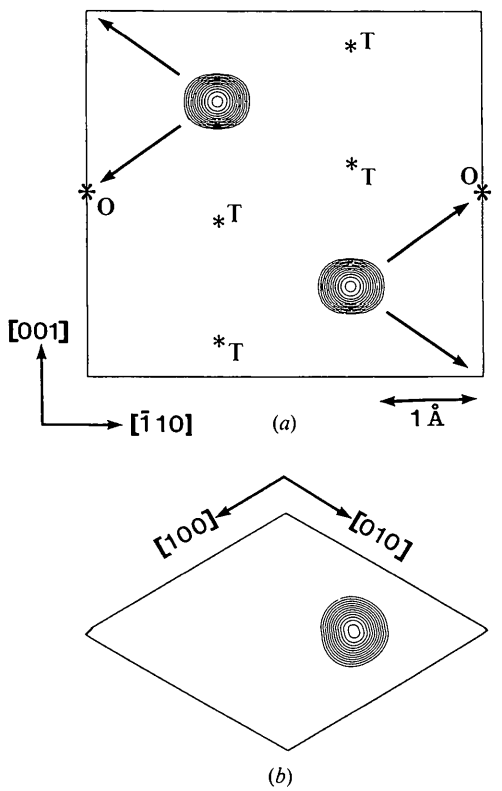

Fig. 1. The MEM nuclear-density distributions of beryllium at room temperature. (*a*) and (*b*) are the (110) and basal planes, respectively. The contour lines are on a logarithmic scale at 0.05 $\times 2.0^n$ ($n = 0, 1, 2, \ldots$) ($\times 10^{-14}$ m Å^{-3}). The tetrahedral and octahedral holes are marked *T* and *O*, respectively.

The atomic thermal motion can be described qualitatively by plots of equipotential contours in a set of planes through the atom. In a study of anharmonic motion in another h.c.p. structure, zinc (Merisalo & Larsen, 1977), it was shown that fourth-order anharmonic terms in the OPP model may deform the equipotential contours from an elliptical shape to one with squarish shoulders in the (100) and (110) planes. The beryllium MEM nuclear density in Fig. 1(*a*) shows significant deviations from the harmonic elliptical shape. By analogy with zinc, the squarish-shoulders feature may be interpreted as resulting from significant quartic anharmonic terms in the OPP function.

In the conventional approach based on least-squares refinement of structure factors, it is very difficult to prove the existence of a quartic anharmonic term because there is usually very high correlation between second- and fourth-order parameters. So far, definitive evidence for fourth-order anharmonicity in beryllium has not been obtained. The squarish shoulders in Fig. 1(*a*) strongly suggest fourth-order anharmonic vibrations. By further analysis of the MEM nuclear-density distribution, it should be possible to determine potential parameters, which describe the thermal atomic displacements of the point nuclei.

4. Nuclear density by the OPP model

The MEM nuclear density gives a picture of the atomic thermal displacements unimpaired by electronic features like chemical bonding or lone-pair electron distributions. The MEM nuclear density will therefore be regarded as the thermal smearing function, also known as the probability density function (p.d.f.), for the nuclei. For an assembly of simple harmonic oscillators, the p.d.f. is a Gaussian function of the displacement, $\langle u^2 \rangle$. As indicated by Willis & Pryor (1975), the root-mean-square atomic displacement in the harmonic case can be derived directly as the half-width at half-peak-height of the p.d.f.

The present case of beryllium is obviously not simple harmonic. It is possible to evaluate the

potential parameters for an anharmonic description of the atomic themal displacements of the point nuclei. In this study, an effective one-particle potential, is assumed to describe the vibrations of beryllium in real space. Potential parameters are determined by three-dimensional function fitting of the OPP model to the real-space MEM nuclear densities.

As mentioned in § 3, thermal-motion effects up to fourth-order anharmonic vibration are found in the MEM nuclear density of beryllium. Therefore, the OPP formalism for the h.c.p. structure is developed up to the fourth-order anharmonic terms, in consideration of the $\bar{6}m2$ site symmetry of beryllium. The OPP can be written

$$\begin{aligned} V(u_1,u_2,u_3) = {} & \beta_1(u_1^2 + u_2^2) + \beta_2 u_3^2 && \text{harmonic term} \\ & + \gamma(u_1^3 - 3u_1u_2^2) && \text{cubic term} \\ & + (\alpha_{40}/8)(3u_1^4 + 3u_2^4 + 8u_3^4 + 6u_1^2u_2^2 \\ & - 24u_1^2u_3^2 - 24u_2^2u_3^2) \\ & + (\beta_{20}/2)(-u_1^4 - u_2^4 + 2u_3^4 - 2u_1^2u_2^2 \\ & - 2u_1^2u_3^2 - 2u_2^2u_3^2) \\ & + \gamma_{00}(u_1^4 + u_2^4 + u_3^4 + 2u_1^2u_2^2 + 2u_1^2u_3^2 \\ & + 2u_2^2u_3^2), \end{aligned} \tag{1}$$

where u_1, u_2 and u_3 are unit vectors along $\langle 210\rangle$, $\langle 010\rangle$ and $\langle 001\rangle$, β_1 and β_2 are the harmonic force constants, γ is the third-order anharmonic parameter (Kurki-Suonio, Merisalo & Peltonen, 1979; Kara & Merisalo, 1982), α_{40} and β_{20} are the fourth-order anisotropic parameters and γ_{00} is the fourth-order isotropic anharmonic parameter (Merisalo & Larsen, 1977, 1979). With the assumption of the classical high-temperature approximation, the p.d.f., $P(u_1,u_2,u_3)$, is calculated from the potential, $V(u_1,u_2,u_3)$, through the Boltzmann distribution function

$$P(u_1,u_2,u_3) = N\exp[-V(u_1,u_2,u_3)/k_BT], \tag{2}$$

where N is the normalization factor. This function will be fitted to the MEM nuclear densities.

In the conventional method of determining thermal parameters, a temperature-factor expression is calculated by a Fourier transformation of the p.d.f. It is then included in the structure-factor expression used in refining the potential parameters by least-squares methods based on the observed structure factors. In this treatment, an approximation in the expansion of the power series of the term $\exp[-V(u_1,u_2,u_3)/k_BT]$ is usually introduced in the process of calculating the Fourier transformation. The MEM analysis using neutron-diffraction structure factors gives the nuclear p.d.f. in real space. The present procedure of thermal-parameter refinement enables approximations in the calculation of the temperature factor to be avoided. Potential parameters in real space are determined by three-dimensional least-squares fitting of the MEM nuclear density using (2).

5. The results of fitting the MEM map

In order to appreciate the importance of the different contributions to the potential for describing the thermal motion in beryllium, the least-squares fitting was carried out step-wise with an increasing number of tems in the potential expression. In Figs. 2(*a*) and (*b*), close-ups of the observed MEM nuclear density at the atomic position are shown for (001) and (100) sections, respectively.

As a first stage, refinements were made applying only the harmonic terms, β_1 and β_2. The reliability factor is

$$R(\rho^2) = \Sigma[\rho_{\mathrm{MEM}}(\mathbf{u}) - \rho_{\mathrm{cal}}(\mathbf{u})]^2/\Sigma[\rho_{\mathrm{MEM}}(\mathbf{u})]^2,$$

where $\rho_{\mathrm{MEM}}(\mathbf{u})$ is the MEM density and $\rho_{\mathrm{cal}}(\mathbf{u})$ is the nuclear density calculated from the OPP model. The summation is over all pixels of the MEM calculation. In the harmonic model, the R factor was 3.5%. The resulting parameters β_1 and β_2 were 2.6926 (6) and 2.872 (1) eV Å^{-2}, respectively. Corresponding calculated nuclear densities in the (001) and (100) sections are shown in Figs. 2(*c*) and (*d*), respectively. The

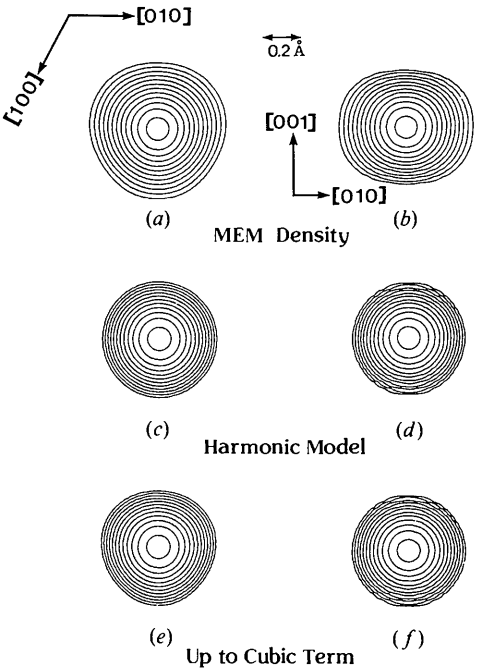

Fig. 2. Close-ups of the MEM nuclear densities and calculated nuclear densities of sections (001) and (100). Contours are as in Fig. 1.

harmonic approximation gives a perfect circular shape in the basal plane and a slightly elliptical shape for the nuclear density in the (100) plane, which is a rather poor approximation to the MEM nuclear density.

In the second stage, the third-order parameter γ was refined, together with the harmonic parameters. The calculated nuclear densities are shown in Figs. 2(*e*) and (*f*) and show good agreement with the MEM nuclear density for the triangular feature in the basal plane. The reliability factor dropped to 3.4%. However, the (100) density still shows an elliptical shape, which is a poor approximation to the MEM density. This implies that the model for the thermal atomic vibration should include fourth-order parameters.

There are three kinds of fourth-order anharmonic parameters. The α_{40} and β_{20} terms describe anisotropic anharmonic vibrations and γ_{00} describes isotropic anharmonic vibrations. To reveal which of these parameters are most important for describing the MEM nuclear density obtained and to relate them to structural features, individual fourth-order parameters were introduced in turn with the harmonic and third-order anharmonic parameters into the least-squares refinement. Parameters and R factors for these refinements are listed in Table 2. Model (1) with the α_{40} fourth-order parameter gives little improvement to the R factor while for model (2), as well as for model (3), the R value drops by 1%.

The effect of the individual fourth-order anharmonic term of the potential can be visualized by drawing the calculated nuclear densities of models (1), (2) and (3). Calculated nuclear densities in the basal plane are almost identical for each model. Those of the (100) plane, on the other hand, show small differences, depicted in Figs. 3(*a*), (*b*) and (*c*) for models (1), (2) and (3), respectively. Judging from the R values of Table 2 and the appearance of the (100) section of the calculated map, the second parameter, β_{20}, has the greatest significance for creating the squarish shoulders. The isotropic fourth-order anharmonic parameter γ_{00} is also very important for a good fit to the (100) MEM nuclear density.

Finally, all thermal parameters, including the three fourth-order terms, were refined in the least-squares process. The calculated nuclear density of (100) with these parameters, shown in Fig. 3(*d*), gives only a marginally improved fit relative to models (2) and (3). The corresponding correlation matrix in Table 3 shows rather high correlation between the fourth-order parameters. On the basis of the significant improvements in R factors, it can be stated that fourth- as well as third-order anharmonic terms are essential for the description of the atomic thermal motion in beryllium metal.

Table 2. *Potential parameters for beryllium with the potential models* (1), (2) *and* (3) *and the final model, which includes all second-, third- and fourth-order parameters*

The last column lists parameters of a previous analysis based on least-squares refinement of structure factors (Larsen *et al.*, 1982)

	Model (1)	Model (2)	Model (3)	Final model	Previous model
β_1 (eV Å^{-2})	2.6922 (6)	2.7902 (5)	2.7556 (4)	2.7755 (4)	2.80 (3)
β_2 (eV Å^{-2})	2.875 (1)	2.7763 (8)	2.9334 (7)	2.892 (1)	3.26 (4)
γ (eV Å^{-3})	−0.442 (6)	−0.340 (5)	−0.341 (4)	−0.306 (4)	−1.0 (3)
α_{40} (eV Å^{-4})	3.73 (7)	0	0	−1.02 (2)	
β_{20} (eV Å^{-4})	0	9.89 (1)	0	2.95 (5)	
γ_{00} (eV Å^{-4})	0	0	−3.926 (3)	−3.28 (2)	
$R\{\rho^2\}$	0.033	0.024	0.022	0.021	

For comparison, room-temperature values of the OPP parameters determined in the study of the temperature dependence of thermal vibrations in beryllium (Larsen, Brown, Lehmann & Merisalo, 1982) are also given in Table 2. In that study, only parameters up to third order were used. The β_1 values agree but the β_2 values differ; however, the correlation matrix shows that the β_2 parameter is correlated rather strongly with the fourth-order parameters β_{20} and γ_{00}, which may conceivably explain the difference.

The problem of high correlation among the thermal parameters can be circumvented by studying integral parameters characterizing the thermal

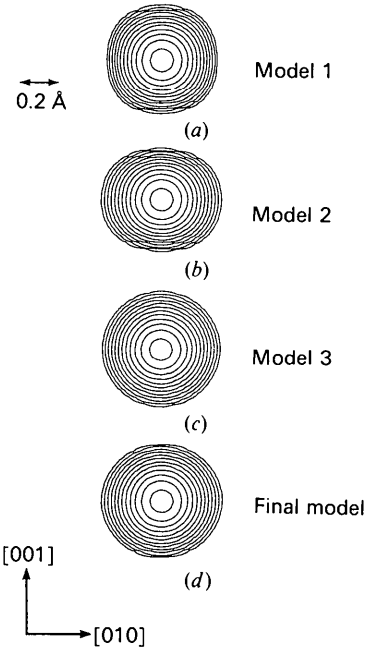

Fig. 3. The (100) nuclear densities calculated with the parameters of models (1), (2) and (3) and the final model in Table 2.

Table 3. *Least-squares correlation matrix for the fit of the final model with all second-, third- and fourth-order parameters*

Second order		Third order	Quartic order		
β_1	β_2	γ	α_{40}	β_{20}	γ_{00}
1.0000	−0.54837	0.16259	−0.03730	0.46060	0.33021
	1.00000	−0.03946	−0.34955	−0.74950	−0.73023
		1.00000	−0.14385	0.12761	−0.07364
			1.00000	0.41276	0.65464
				1.00000	0.93727
					1.00000

smearing function, rather than the harmonic and anharmonic parameters separately. For example, the mean-square amplitudes of the atomic vibrations in the principal directions at the high-temperature limit can be evaluated as an ensemble average by the Boltzmann distribution function, according to (3), where $p = x, z$:

$$\langle u_p^2 \rangle = \sum\{u_p^2 \exp[-V(\mathbf{u})/k_BT]\}/\sum \exp[-V(\mathbf{u})/k_BT]$$
$$= \sum\{u_p^2[\rho_{\mathrm{MEM}}(\mathbf{u})/N]\}/\sum[\rho_{\mathrm{MEM}}(\mathbf{u})/N]. \quad (3)$$

The calculated values are listed in Table 4 next to results obtained by previous conventional least-squares refinement based on structure factors (Larsen, Lehmann & Merisalo, 1980). The present values are slightly smaller than those of the previous analyses, perhaps because fourth-order anharmonic effects are now specifically accounted for.

It should also be noted that the relative magnitudes of the fourth-order parameters are the same as those determined in the study of anharmonicity of lattice vibrations in zinc by neutron diffraction (Merisalo & Larsen, 1979). We are undertaking MEM analyses of single-crystal neutron diffraction data for other h.c.p. metals of different c/a ratios, notably magnesium and zinc, in order to test if this pattern is generally valid.

The significant third-order parameter γ is consistent with the Larsen, Lehmann & Merisalo (1980) result and similar to that for other h.c.p. metals, magnesium (Järvinen, Soininen & Merisalo, 1987) and zinc (Merisalo, Järvinen & Kurittu, 1978; Merisalo & Larsen, 1979). It implies axial anisotropy of vibrations relative to the hexagonal axis. The beryllium MEM neutron-density distribution indicates excess of thermal movement along the $\langle \bar{1}10 \rangle$ directions in the basal plane, which means that the α_{33} term is negative. The existence of the very sizable fourth-order parameter β_{20} shows that the anharmonic softening of the OPP is directed against the octahedral vacancies in the h.c.p. structure.

6. Standard deviations

The standard deviations given in Table 2 for the present calculations are an unrealistically small measure of the total error in the parameter. They are solely measures of how well the least-squares procedure has fitted the model in question to the MEM density distribution. No account is given of the added uncertainty of the parameters, which must reside in the reliability of the MEM density distribution obtained. Presumably, the MEM derives the most likely density distribution from the experimental observations. However, no straightforward measure of precision of the solution obtained is offered at the present stage of development of the technique. The results of the previous studies of the beryllium neutron diffraction data based on least-squares refinements of the structure factors indicate that the parameter values given here are probably reliable to the second digit after the decimal point for the harmonic parameters, β_1 and β_2, and to only the first digit after the decimal point for the anharmonic parameters.

Table 4. *Comparison of mean-square amplitudes of vibration determined from the MEM nuclear density and the previous result*

	MEM nuclear density	Previous study (Larsen *et al.*, 1980)
$\langle u_x^2 \rangle$ (Å^2)	0.00564	0.00594 (3)
$\langle u_z^2 \rangle$ (Å^2)	0.00494	0.00537 (3)

7. Comparison with the MEM electron density

Neutron and X-ray diffraction studies frequently give complementary information. For example, the influence of atomic thermal motion on the X-ray structure factors can be more reliably separated from electronic features when the nuclear positions and their thermal motion have been determined independently from an analysis of neutron diffraction data.

For beryllium, the MEM electron-density distribution based on X-ray powder data was given by Takata, Kubota & Sakata (1993). 19 reflections with $\sin\theta/\lambda < 1.41$ Å^{-1} were available. In order to have the MEM electron-density distribution with resolution similar to Fig. 1, the MEM electron-density map has been calculated from the single-crystal X-ray data of Larsen & Hansen (1984) and is shown in Fig. 4. The planes are the same as in Fig. 1. The contours are drawn on a linear scale only for the lower density region, in order to show better the modulation of the electron-density distribution in the interatomic region. The core electrons around atomic positions stand out like the MEM nuclear density in Fig. 1 but the electron-density distribution is more diffuse and structured in the interatomic region.

There is a local maximum of electron density in the bipyramidal space of two neighboring tetrahedral voids. This must be a purely electronic feature

characteristic of the bonding in beryllium metal, since the MEM nuclear density shown in Fig. 1 has no density outside the atomic positions. Comparison of the MEM nuclear and electron densities indicates that the MEM nuclear-density peak is localized more sharply around the atomic site than that of the MEM electron density.

The electron-density distribution has a slightly triangular shape in the basal plane. The direction of the distortion is opposite to that observed in the MEM nuclear density. Therefore, this deformation in the electron density must be interpreted as an effect of the valence-electron charge density. Similar oppositely directed deformations in nuclear- and electron-density distributions caused by anharmonic motion and bonding-electron redistribution have also been mentioned for the diamond structure by Willis & Pryor (1975). The asymmetric surrounding of an atom, which sees a nearest neighbor in one direction and a hole in the structure in the opposite direction, causes anharmonic motion of the nucleus such that the atom spends more time towards the hole than towards the bond. Thus, the tetrahedral anharmonic deformation is oppositely directed to the tetrahedral bonding distribution.

For beryllium metal in the h.c.p. structure, the nuclear-density distribution is deformed towards the octahedral voids; Fig. 4 shows that the electron-density distribution is deformed in the basal plane towards the bipyramidal space around the tetrahedral holes.

There is a local maximum in the electron density centered between three neighboring atoms in the basal plane of the h.c.p. structure. We are presently carrying out a topological analysis of the MEM electron density in beryllium according to Bader's (1990) scheme. The topological analysis characterized this point as a non-nuclear attractor. Details of the MEM electron-density-distribution study will be reported in a forthcoming paper.

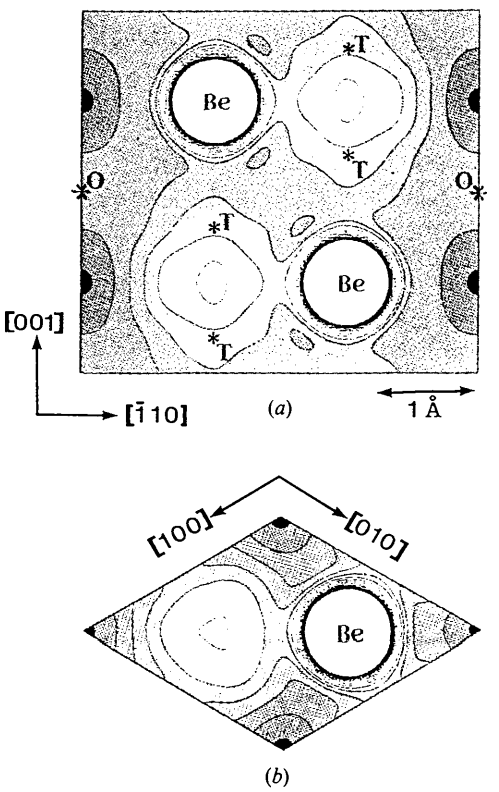

Fig. 4. The MEM electron-density distributions of beryllium at room temperature based on X-ray single-crystal diffraction data. (*a*) and (*b*) are the (110) and basal planes, respectively. The contours are from 0.0 to 2.0 at intervals of 0.05 e $Å^{-3}$ on a linear scale. The tetrahedral and octahedral holes are marked *T* and *O*, respectively.

8. Concluding remarks

This study shows that the MEM based on neutron diffraction data can reveal even small anharmonic thermal effects in a crystal. Direct fitting of the MEM nuclear density by the OPP model is a powerful new method that can determine a precise value for the force constants of the harmonic and anharmonic terms of the potential. This method has the great advantage of making possible a direct judgment of the appropriate model for describing the thermal motion in real space. The MEM analysis gives rich information about the nature of anharmonic motion in beryllium without involving any structural model for the atomic thermal motion.

The authors thank Professor J. Danielsen for his kind help with the computational work. The authors also thank Professors J. Harada and S. E. Rasmussen for their encouragement. Most of the computations were carried out at the Computer Centre of Nagoya University, which is gratefully acknowledged by the authors. The authors thank the Computer Centre of the Department of Chemistry of Aarhus University for the use of the workstations, the personal DECstation 5000 and the IRIS Indigo. This work has been partly supported by a Grant in Aid of Scientific Research from the Ministry of Education, Science and Culture of Japan and by the Danish National Science Research Council.

References

BADER, R. F. W. (1990). *Atoms in Molecules. A Quantum Theory.* Oxford: Clarendon Press.

COLLINS, D. M. (1982). *Nature (London)*, **298**, 49–51.

JÄRVINEN, M., SOININEN, J. & MERISALO, M. (1987). *Acta Cryst.* A**43**, 694–698.

KARA, M. & MERISALO, M. (1982). *Philos. Mag.* B**45**, 25–30.

KUMAZAWA, S., KUBOTA, Y., TAKATA, M., SAKATA, M. & ISHIBASHI, Y. (1993). *J. Appl. Cryst.* **26**, 453–457.

KURKI-SUONIO, K., MERISALO, M. & PELTONEN, H. (1979). *Phys. Scr.* **19**, 57–63.
LARSEN, F. K., BROWN, P. J., LEHMANN, M. S. & MERISALO, M. (1982). *Philos. Mag.* B**45**, 31–50.
LARSEN, F. K. & HANSEN, N. K. (1984). *Acta Cryst.* A**40**, 169–179.
LARSEN, F. K., LEHMANN, M. S. & MERISALO, M. (1980). *Acta Cryst.* A**36**, 159–163.
MERISALO, M., JÄRVINEN, M. & KURITTU, J. (1978). *Phys. Scr.* **17**, 23–25.
MERISALO, M. & LARSEN, F. K. (1977). *Acta Cryst.* A**33**, 351–354.
MERISALO, M. & LARSEN, F. K. (1979). *Acta Cryst.* A**35**, 325–327.
SAKATA, M., MORI, S., KUMAZAWA, S., TAKATA, M. & TORAYA, H. (1990). *J. Appl. Cryst.* **23**, 526–534.
SAKATA, M. & SATO, M. (1990). *Acta Cryst.* A**46**, 263–270.
SAKATA, M., TAKATA, M., KUBOTA, Y., UNO, T., KUMAZAWA, S. & HOWARD, C. J. (1992). *Adv. X-ray Anal.* **35**, 77–83.
SAKATA, M., TAKATA, M., OSHIZUMI, H., GOTO, A. & HONDOH, T. (1992). *Physics and Chemistry of Ice*, pp. 62–68. Hokkaido Univ. Press, Sappolo, Japan.
SAKATA, M., UNO, T., TAKATA, M. & HOWARD, C. J. (1993). *J. Appl. Cryst.* **26**, 159–165.
SAKATA, M., UNO, T., TAKATA, M. & MORI, R. (1992). *Acta Cryst.* A**39**, 47–60.
TAKATA, M., KUBOTA, Y. & SAKATA, M. (1993). *Z. Naturforsch. Teil A*, **48**, 75–80.
TAKATA, M., YAMADA, M., KUBOTA, Y. & SAKATA, M. (1992). *Adv. X-ray Anal.* **35**, 85–90.
WILLIS, B. T. M. & PRYOR, A. W. (1975). *Thermal Vibrations in Crystallography*. Cambridge Univ. Press.

Acta Cryst. (1994). A**50**, 337–342

Comparison between Experimental and Theoretical Rocking Curves in Extremely Asymmetric Bragg Cases of X-ray Diffraction

BY SHIGERU KIMURA* AND JIMPEI HARADA

Department of Applied Physics, Nagoya University, Chikusa-ku, Nagoya 464-01, *Japan*

AND TETSUYA ISHIKAWA

Department of Applied Physics, University of Tokyo, 7-3-1 *Hongo, Bunkyo-ku, Tokyo* 113, *Japan*

(*Received* 1 *July* 1993; *accepted* 19 *October* 1993)

Abstract

Double-crystal rocking curves from a highly perfect silicon crystal were taken in extremely asymmetric schemes, in which the glancing angles of the incident X-rays were very close to the critical angle of total external reflection. The experimental rocking curves were compared with theoretical calculations based both on an ordinary dynamical theory of diffraction and also on an extended dynamical theory, which uses a more exact solution of the fundamental equation of the dynamical theory and takes the effect of specular reflection into account. It is demonstrated from such a comparison that, in the case of extremely asymmetric diffraction, the ordinary treatment of the dynamical theory of diffraction is not valid; in contrast, the extended theory explains the rocking curve very well.

1. Introdution

Extremely asymmetric Bragg-case diffraction with an incident-beam glancing angle close to the critical angle of total reflection has been a subject of great interest in applications such as the study of surfaces (Kitano, Ishikawa, Matsui, Akimoto, Mizuki & Kawase, 1987; Kitano, Kimura & Ishikawa, 1992; Kimura, Mizuki, Matsui & Ishikawa, 1992) and interfaces (Hasegawa, Akimoto, Tsukiji, Kubota & Ishitani, 1993). Under these conditions, however, ordinary treatments of the dynamical theory of diffraction (Zachariasen, 1945) are not valid, since the effects of specular reflection can no longer be neglected. Consequently, several theoretical studies (Kishino & Kohra, 1971; Bedyńska, 1973; Rustichelli, 1975; Zeilinger & Beatty, 1983; Afanas'ev & Melikyan, 1990) have been reported on diffraction phenomena in such an extremely asymmetric case. According to the work of these authors: (1) the angular deviation from Bragg's law, $\Delta\theta_0$, approaches the critical angle of total reflection, θ_c, as $\theta_B - \alpha$ goes to zero, where θ_B is the Bragg angle and α is the angle between the crystal surface and diffracting planes; (2) the full width at half-maximum (FWHM) of the rocking curve has a maximum value at a small glancing angle and cannot be larger than this maximum value as $\theta_B - \alpha$ becomes even smaller. The ordinary treatment of the dynamical theory, however, shows that both $\Delta\theta_0$ and the FWHM diverge.

* Permanent address: Microelectronics Research Laboratories, NEC Corporation, 34 Miyukigaoka, Tsukuba, Ibaraki 305, Japan.